PROCEEDINGS OF SCIENCE

A Brief Discussion on the Performance of the MoEDAL and the LHCf Experiments

Arka Santra* **on behalf of the MoEDAL and LHCf Collaborations**
Instituto de Física Corpuscular (IFIC), CSIC – Universitat de València,
Parc Científic de la U.V., C/ Catedrático José Beltrán 2,
E-46980 Paterna (Valencia), Spain
E-mail: santra.arka@ific.uv.es

The Monopole and Exotics Detector at the LHC (MoEDAL) experiment is an experiment dedicated to searching for beyond standard model (BSM) particles like magnetic monopoles, highly ionizing particles and slow-moving supersymmetric particles. In many ways, this detector complements the BSM searches of ATLAS and CMS. In this document, a brief description of the MoEDAL detector and performance is given.

The Large Hadron Collider Forward (LHCf) experiment, on the other hand, is dedicated to measuring the neutral particles produced in the hadronic collision in the very forward region. This document also briefly discusses the LHCf detector and its performance.

Sixth Annual Conference on Large Hadron Collider Physics (LHCP2018)
4-9 June 2018
Bologna, Italy

*Speaker.

PoS(LHCP2018)233

1. Introduction

The Monopole and Exotics Detector at the LHC (MoEDAL) [1] [2] is the newest and the 7^{th} experiment at the Large Hadron Collider (LHC) [3]. This experiment was approved in 2010 and it started the data taking in 2015. The research goal of this experiment is to search for new physics through highly ionizing particles [4] complementing the research goals of the ATLAS and CMS experiments. Though the most important motivation for this experiment is to search for magnetic monopoles and dyons at the LHC energies, this is also designed to search for any stable or long-lived, slow moving massive particle messengers of new physics.

The motivation behind the Large Hadron Collider forward experiment (LHCf) [10] is to measure the hadronic production of the neutral particles emitted in the very forward region (pseudorapidity, $|\eta| > 8.4$). The models which predict the forward particle generations in hadronic collisions can be tested by the data collected by the LHCf experiments. These models are critical in the measurement of the properties of extended air showers created by Ultra High Energy Cosmic Rays (UHECRs).

2. MoEDAL Experiment

The MoEDAL experiment is situated around the interaction point of LHC point 8, in the LHCb Vertex Locator (VELO) cavern. The three dimensional diagram of the MoEDAL experiment along with the LHCb experiment is shown in Figure 1. There are three subdetectors contained in this detector, which are described below.

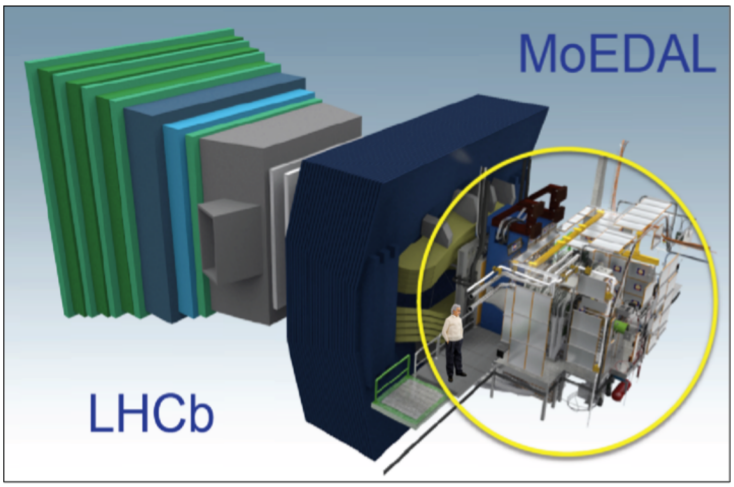

Figure 1: A three dimensional figure of MoEDAL experiment along with the LHCb experiment.

2.1 Nuclear Track Detector

The nuclear track detector (NTD) stacks surrounding the interaction point. This detector is made of a large array of CR39®, Makrofol® and Lexan®. When a highly ionizing particle passes through the NTDs, it leaves invisible tracks inside the polymer chain of the plastic (Figure 2). These

invisible tracks can be made visible by the chemical etching process. For the chemical ething, the etchant used are 6N/8N NaOH, 6N/8N KOH etc. It has been found that the bulk etch rate (v_B) increases with the increase of the temperature and the presence of alcohol in the etchant mixture [5]. The threshold of MoEDAL NTDs is $Z/\beta \sim 5$ where Z is the electric charge of the particle and β is the velocity of the particle in units of c, the speed of the light. Exposed NTDs are scanned through automated high rate CCD based scanning microscope developed by the groups at Bologna, Muenster and Helsinki (etch-pit size $\sim 30\ \mu$m).

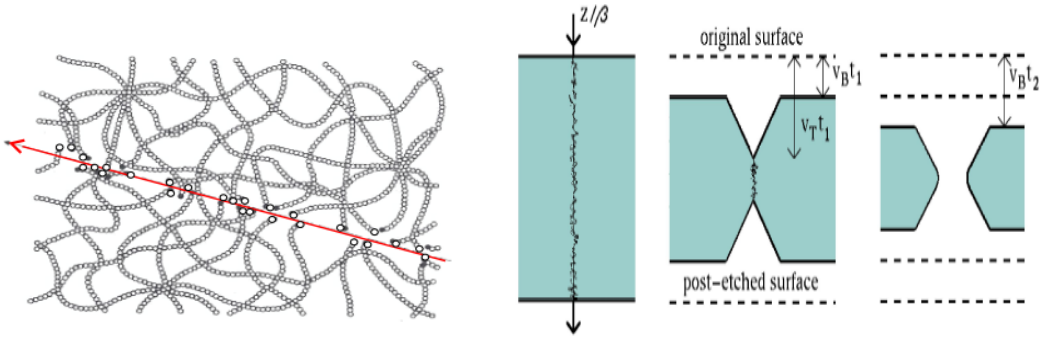

Figure 2: The invisible tracks made by the highly ionizing particles (left) are made visible by chemical etching. The NTD, before and after chemical etching process is shown in the right hand side figure.

2.2 Magnetic Monopole Trappers

The magnetic monopole trapper (MMT) of the MoEDAL detector is made of array of paramagnetic aluminium bars. Since aluminium has anomalously high nuclear moment, it is used to capture the electrically and magnetically charged highly ionising particles. For the 2015 run at the 13 TeV, there were 672 square aluminium rods with dimension $19 \times 2.5 \times 2.5$ cm^3 for a total mass of 222 kg in 14 stacked boxes (MMT1) placed 1.62 m from the interaction point. In 2017, two more MMTs (MMT2 and MMT3) with mass 286 kg each were placed parallel to the beam pipe. The present deployment of the MMTs is shown in Figure 3.

The exposed MMTs are taken to a remote SQUID magnetometer facility to check if the MMTs trap any highly ionizing particle [6] [7]. The details of the calibration of the SQUID magnetometers can be found elsewhere [6].

When the MMT sample is passed through the SQUID Magnetometer, there is an induced current. When the sample contains no magnetic monopole no current should be registered. However, if the sample is contaminated with ferromagnetic material, it will act like a magnetic dipole. So, a current will be generated while the sample is passing though the coil, but, there will be no net current flowing in the coil after the sample has passed though the coil. If there is a magnetic monopole trapped in the MMTs, there will be a persistent induced current in it (Figure 4).

2.3 TimePix Radiation Monitors

The TimePix radiation monitors are the only active component of the MoEDAL detector. They are composed of pixel device arrays (256×256 square pixels with a pitch of 55 μm). Each pixel has the TimePix chip which consists of a preamplifier, a discriminator with threshold adjustment, synchronizing logic and a 14-bit counter [8].

2.4 MoEDAL Resolution and Sensitivity

For the NTDs, the tracking resolution is 10 μm/etched pit. The pointing resolution to the interaction point is around 1 cm. The charge resolution is 0.1 times the unit of the electric charge (e).

In the trapping detector (MMT), the magnetic charge resolution is less than 0.1 $g_{\rm D}$, where $g_{\rm D}$ is the unit of Dirac charge and has an equivalent value of 68.5e. For the TimePix chips, the pixel size is 55×55 mm^2.

The MoEDAL detector has low energy threshold compared to other LHC experiments (ATLAS, CMS, ALICE and LHCb) with full angular coverage. For MoEDAL, the luminosity is medium and the efficiency is robust.

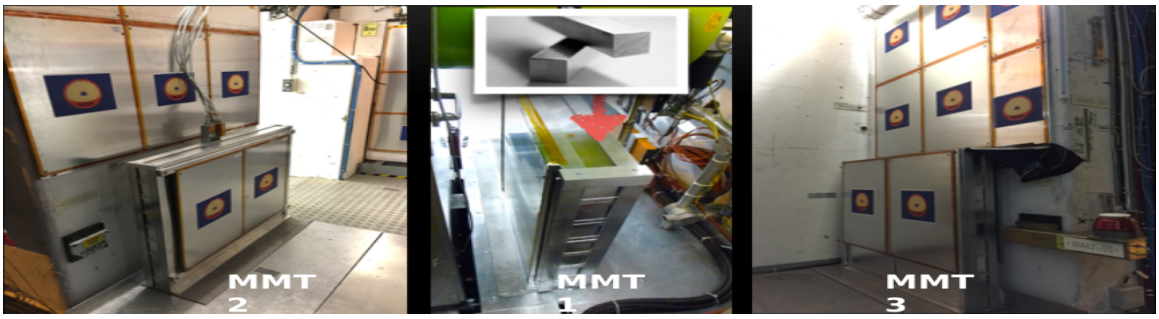

Figure 3: The images of different MMTs. In the inset, one can see the square aluminium rods which go inside the MMT.

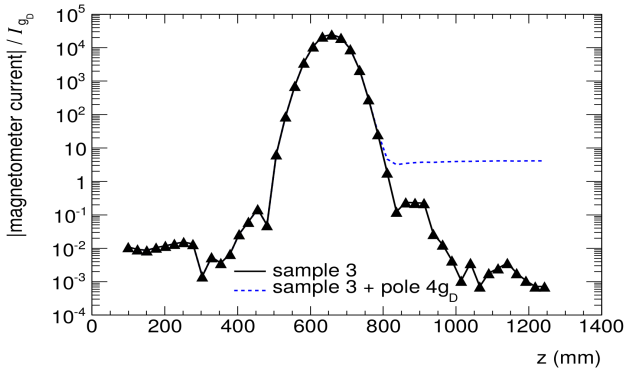

Figure 4: The response (i.e. current) of the SQUID magnetometer when a beampipe sample 3 (with no magnetic monopole trapped in it) is passed through it as a function of z. In this figure, the blue dashed line shown is the signature if the beampipe sample carry a magnetic charge of 4.14 $g_{\rm D}$, $g_{\rm D}$ being the Dirac magnetic charge. The unit of the y axis is the magnetometer current in terms of current expected from a Dirac monopole (I_{g_D}).

3. LHCf Experiment

Two independent detectors, Arm1 and Arm2 make the LHCf detector. They are installed at $\pm$140 m from the interaction point of ATLAS. The Arm1 detector has two calorimetric towers

where first tower covers the pseudorapidity (η) region of > 10 and the second tower covers the region $8.5 < \eta < 9.5$. The calorimeter tower dimension is 20×20 mm^2 and 40×40 mm^2 respectively.

Each tower is made of 16 sampling layers and four position sensitive layers interleaved in the tungsten absorbers. For the sampling layers Gd_2SiO_4 scintillators (GSO) are used, one of the best inorganic scintillators at present. The position sensitive layers for Arm1 are the hodoscope layers are made of GSO bars. The position sensitive layers for Arm2 are the silicon strip sensors. The first half of the calorimeter has sampling layers at every two radiation lengths (X_0), because this part is mainly used for electromagentic (EM) shower development. In the second half, the sampling layers are at every four radiation lengths, which is used mainly for hadronic showers. The total length of each calorimeter is $44X_0$. The leakage from the EM shower is really negligible at the back of the tower. The schematic diagrams of each of the towers are shown in Figure 5 [11].

With this configuration, the energy resolution for photons (with energy higher than 100 GeV) becomes less than 5%. The energy resolution for the neutrons is roughly 40%. The position resolution of the photons is less than 200 μm, but for neutrons, it is a few mm.

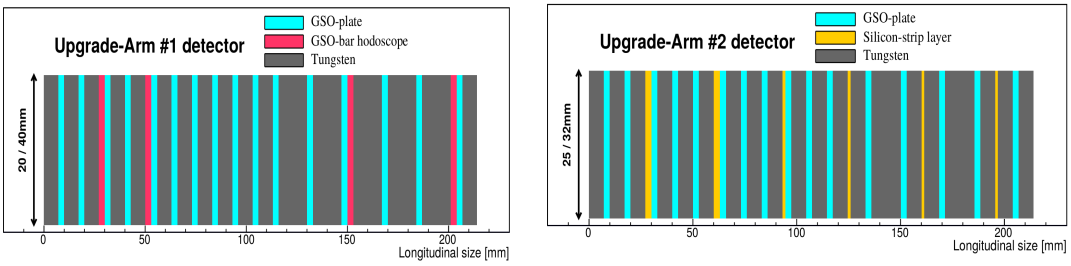

Figure 5: The schematic diagram of Arm1 (left) and Arm2 (right) calorimeter towers of LHCf detector. One can see the sampling layers in the first half are placed at $2X_0$, where X_0 is the radiation length, where as for the second half, the sampling layers are kept at $4X_0$.

The particle identification estimator distribution from the LHCf detector is shown in Figure 6. In this figure, the data obtained match quite well the simulation of electromagnetic shower in the shallow layers, and simulation of hadronic shower in the deep layers. The good agreement between data and simulation shows the good understanding of the detector and it is also used for estimation of efficiency and contamination.

The preliminary results of neutron energy spectra for proton-proton collisions at $\sqrt{s} = 13$ TeV are shown in Figure 7 [12].

4. Conclusions and Outlook

A brief discussion of the MoEDAL and LHCf experiments is given here. In 2018, MoEDAL published its most recent results on the magnetic monopole search, with 2.11 fb^{-1} of data [9]. MoEDAL is presently taking the data and new results will be published soon. Apart from the search for magnetic monopoles, it is also searching for Heavy Electrically Charged Objects that include slowly moving supersymmetric particles.

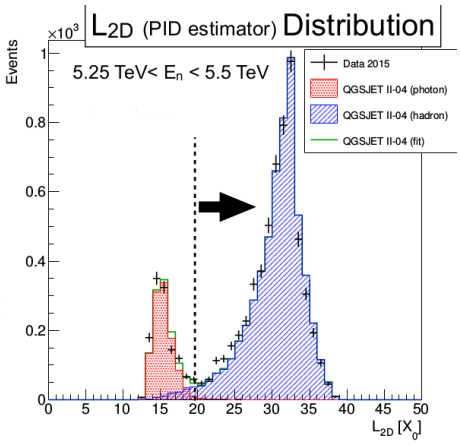

Figure 6: The longitudinal shower shapes L_{2D} in terms of radiation length X_0 in the calorimeter from data and simulation are shown. The good agreement of data and simulation shows a good understanding of the detector. Here E_n is the reconstructed neutron energy.

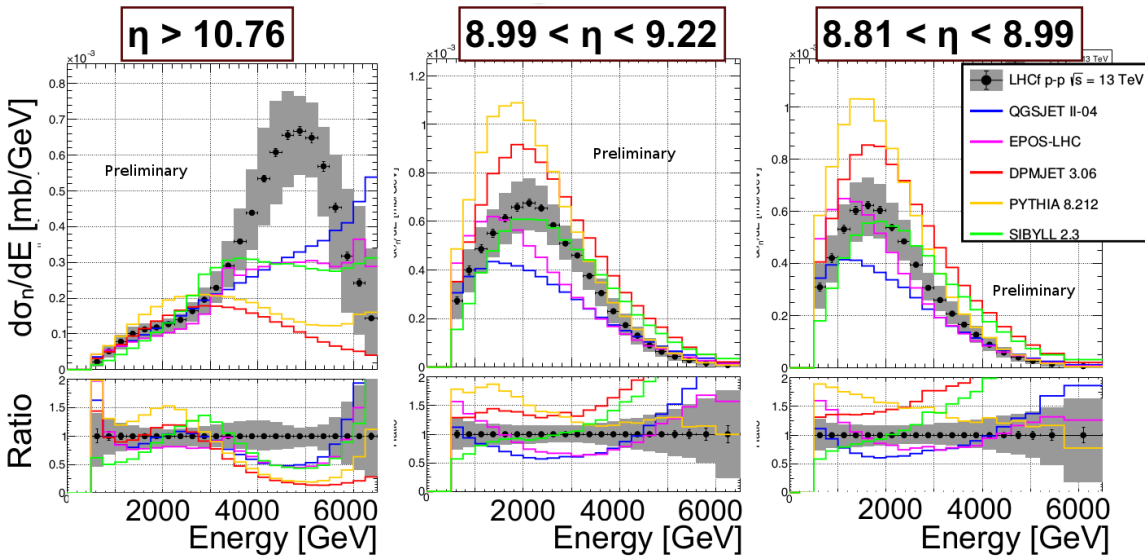

Figure 7: The preliminary results of neutron energy spectra for proton-proton collisions at $\sqrt{s} = 13$ TeV. The data are compared with QGSJet II-04, EPOS-LHC, DPMJet 3-0.4, PYTHIA 8.212 and SIBYLL 2.3 generators.

LHCf measured the neutron cross-section in the proton-proton collision at $\sqrt{s} = 13$ TeV. ATLAS and LHCf jointly worked on the contribution of diffractive processes to the forward particle production [13]. In future, there is a discussion going on in order to get collision with proton and oxygen at the LHC, which gives the ideal condition for the cosmic rays. Also it will measure the forward π^0 and η production cross-section at the proton-proton collision with $\sqrt{s} = 13$ TeV.

5. Acknowledgement

The author acknowledges the support by the Generalitat Valenciana (GV) through the MoEDAL-supporting agreement CON.21.2017-09.02.03 and by the Spanish MINEICO under the project FPA2015-65652-C4-1-R. This work is also supported by the Severo Ochoa Excellence Centre Project SEV-2014-0398.

References

[1] For general information on the MoEDAL experiment, see: http://moedal.web.cern.ch/

[2] MoEDAL Collaboration, Technical Design Report of the MoEDAL Experiment CERN Preprint CERN-LHC-2009-006, MoEDAL-TDR-1.1 (2009), and references therein.

[3] L. Evans and P. Bryant, JINST 3, S08001 (2008).

[4] M. Fairbairn, A. C. Kraan, D. A. Milstead, T. Sjostrand, P. Z. Skands and T. Sloan, Phys. Rept. 438, 1(2007); S. Burdin, M. Fairbairn, P. Mermod, D. Milstead, J. Pinfold, T. Sloan and W. Taylor, Phys. Rept. 582, 1 (2015).

[5] MoEDAL Public webpage: https://moedal.web.cern.ch/content/etching-process.

[6] M. D. Joergensen, A. De Roeck, H.-P. Hachler, A. Hirt, A. Katre, P. Mermod, D. Milstead and T. Sloan, "Searching for magnetic monopoles trapped in accelerator material at the Large Hadron Collider," arXiv:1206.6793 [physics.ins-det] (2012).

[7] A. De Roeck, H. P. Hachler, A. M. Hirt, M.-D. Joergensen, A. Katre, P. Mermod, D. Milstead and T. Sloan, Eur. Phys. J. C 72, 2212 (2012).

[8] V. A. Mitsou [MoEDAL Collaboration], "Searches for magnetic monopoles and beyond with MoEDAL at the LHC," EPJ Web Conf. **181**, 01030 (2018). doi:10.1051/epjconf/201818101030.

[9] B. Acharya *et al.* [MoEDAL Collaboration], "Search for magnetic monopoles with the MoEDAL forward trapping detector in 2.11 fb^{-1} of 13 TeV proton-proton collisions at the LHC," Phys. Lett. B **782**, 510 (2018) doi:10.1016/j.physletb.2018.05.069 [arXiv:1712.09849 [hep-ex]].

[10] LHCf collaboration, "The LHCf detector at the CERN Large Hadron Collider", 2008 *JINST* **3** S08006.

[11] Y. Makino *et al* "Performance study for the photon measurements of the upgraded LHCf calorimeters with Gd_2SiO_5 (GSO) scintillators", 2017 *JINST* **12** P03023.

[12] E. Berti and A. Oscar, "Measurement of the energy spectra relative to neutrons produced at very small angle in $\sqrt{s} = 13$ TeV proton-proton collisions using the LHCf Arm2 detector", CERN-THESIS-2017-035, https://cds.cern.ch/record/2262680.

[13] The ATLAS and LHCf Collaboration, "Measurement of contributions of diffractive processes to forward photon spectra in pp collisions at $\sqrt{s} = 13$ TeV", ATLAS-CONF-2017-075.